This CUME is based on the accompanying paper McIntosh et al, 2017, Nature, 1, 0086 "The detection of Rossby-like waves on the Sun" This is quite a short paper with 4 main figures and some supplementary material Attempt all questions.

There are 50 total points available.

A total of 35 points is *expected* to be a passing grade.

Do not allow yourself to get stuck on any one question.

I suggest you try to get through all questions inside the first hour and then use the second hour to go back and complete any parts you have skipped.

Calculators are only to be used for calculations. You may not store equations. You may not use your cell phone at any time.

Show all work for full points. Attempt all parts of all questions.

Take a new page for each question. This makes it much easier to award partial credit for incorrect answers.

			ı
			·
	,		

- 1. Lets discuss the ideas presented in this paper.
 - (a) Summarize the main 3-4 results of this paper, and the implications of these. (I'm looking for a short paragraph or bullet list)

3 points

(b) In 2-3 sentences, describe the effect of the Coriolis force on Earth at a level that could be understood by someone with a physics degree. Include a clear, annotated figure to show the effect of Coriolis force on material moving away from, and towards, the equator in both hemispheres (both northward and southward)

7 points

- 2. Consider a body moving with velocity v, in the atmosphere of body that is rotating with angular frequency Ω . The acceleration due to the Coriolis force on this body is given as $2\Omega \times v$.
 - (a) What does this imply about the direction of the Coriolis force

3 points

(b) If the Coriollis acceleration and centripetal acceleration are equal, derive the equation for Coriolis frequency as

$$\omega = 2 \Omega \sin(\phi)$$

where ϕ is latitude.

7 points.

3. The Rossby parameter is the gradient of the Coriolis frequency across latitude. $\beta = \nabla \, \omega$

As
$$\nabla = \hat{\mathbf{r}} \frac{\partial}{\partial r} + \frac{1}{r} \hat{\boldsymbol{\phi}} \frac{\partial}{\partial \phi} + \frac{1}{r \sin \phi} \hat{\boldsymbol{\theta}} \frac{\partial}{\partial \theta}$$

(a) Derive the equation for the Rossby parameter at some radial distance a, as $\beta = (1/a) \ (2\Omega \cos (\phi)$

3 points

(b) And show that at the tachocline (a_t=0.7Rsun), at a mid latitude of 45 degrees $\beta_t \sim 8 \times 10^{-15}\,\text{m}^{-1}~\text{s}^{-1}$

7 points

4. The angular frequency of a Rossby wave can be calculated as $\omega = (-\beta_t) / (2\pi k)$, and the typical wavelength of these features are about 75Mm. Show that the typical timescales for these features is similar to those discussed in the paper

"The rotational timescale dependence of BP cluster emergence and lifetimes found here also ties the present analysis to the modulation of solar activity on timescales of years and months⁶. "

2

The rotation period of the Sun at the tachocline is about 25 days. The radius of the Sun is 7 x 10^{10} cm

5 points

5. The observational determination of the phase velocity is described on page 3 and page 4, with reference to the supplementary figures.

"(velocity = $\tan \theta$ = range of cluster longitude / cluster lifetime; a velocity in radians per year is easily converted into metres per second)"

Carry out this calculation to the data in figure 3 to obtain the phase velocity of around 3ms⁻¹ as derived in the paper

5 points

6. The paper claims that "Indeed, a theoretical relationship between the toroidal magnetic field strength at the bottom of the solar convection zone and the 3 m s⁻¹ phase velocity of the magnetized Rossby waves⁵ would yield magnetic field strengths of the order of 4 kG, consistent with that measured in the strongest of sunspots¹⁹.

From reference 5 (Zaqarashvili et al. 2015) I obtained the following relationship for the phase velocity at the tachocline (in cgs units).

$$v_{\rm ph} = -\frac{B_0^2}{4\pi\rho\Omega_0R} \frac{2-n(n+1)}{2},$$

where Bo is the magnetic field at the tachocline, $\rho_0 = 0.2$ g cm⁻³, Ω_0 and R are as above. Show this statement is only true for a low poloidal wave number, n n is the poloidal wave number (i.e, number of convective cells in latitude)

10 points

CI) 9
ROSS BY NAMES ON SON, SIMICAR TO PRAMESS

PHASE VELOCITIES AND GRACED VELOCITIES

ABREE WITH PREDICTIONS

LEADS TO PERIODS, B, de THAT OCCUR

ON THE SUN

ASSIST WHI LONG TERM UNDERSTANDNE

CF SPACE CLIMPATE

MANN PROTS - TOPIC IS WANTS

- PERCESS WITH EXPRESSION AND LEADS TO MANN VALUES

			4
		•	
· ·			
			١
			,

ACTS ON OGSTETS IN MOTION RELATIVE TO ROTATIVE REFERENCE

· MERTIAZ (PSEUDO) FORCE

· RESULTS FROM OPTIMENT SPETIOS AT

nex / 4

STOCKT EXHIBITS EXCERCENT, COHERENT WRITTEN DESCRIPTION STUDENT EXHIBITS SOME INFORMET BARRYSIS, OR INCOHEMENT 2 STUDENT EXHIBITS MANY SENERE MISCONCEPTUNS OR POOR DESCRIPTION CCEAR, ANDONATED COMPRESE FRANCE SHOWNE DASIC CONFEDER 16/2= / 3 MESSY, INCOMERCIA, OR INCOMPLETE FIEURE

					¥,
	,				
,					

(5) (3) CORIOLIS ACCERCICION = 2 12 X = 2 12 W sin P COMPONENT) HOVE120NJA (CONSIDERING CEMPIFOAL SCERETATION V? PW = W 57 = 2 12 / sin 4 =2 52 sin p W=21250P

Ceriais Accerement WILL DE PERP TO BOTH ROTATION AXIS AND ROTATION AXIS (9)

DERLATION COMPLETES OFFICENTION STUDENT SETS EQUATIONS FROM DUT DOES NOT COMPLETE STUDER GETS BOTH FRATION OUT DAS NOT SET ELA STUCK anner Eepur STUTEM TEXT DOG NOT DISCUSS I TO ROTATION

AXIS OR J

				•
		·		
	•			

B = 7W $= \frac{1}{7} \frac{2}{84} 2 \cdot 5 \cdot n \cdot 4$ $= \frac{2}{7} \frac{2}{60} \cos \theta$

STUDER COMPLETES DERIVATION 3
STUDER REQUIES 'GRAD' BG MANTS I GRADE Z
STUDEN CAMPOR COMPLETE DERIVATION

٠

(3) 9

		· 15

$$\beta = \frac{1}{a} 2 \Omega \cos \theta$$

$$= \frac{2}{a} \frac{2\pi}{T} \cos 4 S$$

$$= \frac{2}{a} \frac{2\pi}{T} \cos 4 S$$

$$= \frac{2\pi}{28 \times 8.5 \times 10^{4}} \frac{1}{9\pi \times 7 \times 10^{8}} \frac{0\pi}{25 \times 8.5 \times 7} \times 10^{8}$$

$$= \frac{4\pi}{2.5 \times 8.5 \times 7} \times 10^{11} \frac{11118}{2.5 \times 8.5$$

				9
		:		
,				

$$P = \frac{211}{1 \text{ w}}$$

$$AWW = \frac{211}{214 \text{ k}}$$

$$AWW = \frac{211}{214 \text{ k}}$$

$$2 k = \frac{2\pi}{75 \times 10^6}$$

$$\approx 0.08 \times 10^{-6}$$

$$\approx 8 \times 10^{-8}$$

$$\approx 8 \times 10^{-15}$$

$$\approx 2\pi (.8 \times 10^8)$$

$$\approx -0.16 \times 10^{-8}$$

$$\approx -0.16 \times 10^{-8}$$

$$P = \frac{2\pi}{|w|} = \frac{2\pi}{1.6 \times 10^{8}}$$

$$\sqrt{3.9 \times 10^{8}} = \frac{5}{1.6 \times 10^{8}}$$

$$\sqrt{1.0} = \frac{5}{1.6 \times 10^{8}}$$

ERRORS: CALCUME K -2 CALCUAN W -2 CALCUAN P -1

			. •
y			
		× .	
	**; 		

OT
$$Q = 0^{\circ}$$
 $C = 2\pi R = 2\pi (7 \times 10^{8}) = 44 \times 10^{8}$ M
AT $Q = 15^{\circ}$, CIRCHARGAGAGAGAGA SON IS LILE XIO COS IS
$$= 42.5 \times 10^{8} \text{ M}$$

VERDCITY =
$$\frac{10}{360} \times 42.5 \times 10^8$$

1.58 × 10

20.75 × 10

=7.5 M 5

LOOUING FOR A CAPACITE OF CAPACITE CA

STATE COLD ESTABLE DEGREES NOTE POORCY

OMIT COMBASION AT 15°

NOTHER METICAL EXPRONT

UNT ERRONT

EXECT LARGE RANGE OF VALUES

		e u
·		

(6)

ENRON

INPOT

		Y		

PUBLISHED: 27 MARCH 2017 | VOLUME: 1 | ARTICLE NUMBER: 0086

The detection of Rossby-like waves on the Sun

Scott W. McIntosh^{1*}, William J. Cramer², Manuel Pichardo Marcano³ and Robert J. Leamon⁴

Rossby waves are a type of global-scale wave that develops in planetary atmospheres, driven by the planet's rotation1. They propagate westward owing to the Coriolis force, and their characterization enables more precise forecasting of weather on Earth^{2,3}. Despite the massive reservoir of rotational energy available in the Sun's interior and decades of observational investigation, their solar analogue defies unambiguous identification⁴⁻⁶. Here we analyse a combined set of images obtained by the Solar TErrestrial RElations Observatory (STEREO) and the Solar Dynamics Observatory (SDO) spacecraft between 2011 and 2013 in order to follow the evolution of small bright features, called brightpoints, which are tracers of rotationally driven large-scale convection. We report the detection of persistent, global-scale bands of magnetized activity on the Sun that slowly meander westward in longitude and display Rossby-wave-like behaviour. These magnetized Rossby waves allow us to make direct connections between decadal-scale solar activity and that on much shorter timescales. Monitoring the properties of these waves, and the wavenumber of the disturbances that they generate, has the potential to yield a considerable improvement in forecast capability for solar activity and related space weather phenomena.

Coronal brightpoints (BPs) permit the tracking of the magnetic activity bands of the 22-year magnetic cycle of the Sun8. These activity bands in each solar hemisphere undergo significant quasi-annual instability, which results in episodes of intensified space weather6. The nature of the instability on the bands is unknown, but has been linked to the existence of magnetic Rossby waves in the solar interior⁵. We use our BP detection algorithm⁹ on a series of coronal images taken by the Extreme-Ultraviolet Imager (EUVI) instruments¹⁰ on the twin STEREO spacecraft, and by the Atmospheric Imaging Assembly (AIA) instrument¹¹ on the SDO spacecraft, in the 19.5- and 19.3-nm channels, respectively, from 1 June 2010 to 31 May 2013. During this time period, the orbits of these three spacecraft created an opportunity to explore global-scale solar phenomena. In concert, the trio of spacecraft provided the first complete observational coverage of the Sun's corona, slowly drifting apart from the Sun-Earth line until STEREO-Behind lost communication with the Earth in mid-2014.

Figure 1 shows an example of BP detection for the three spacecraft on 2 February 2011 in these channels, which are highly sensitive to emission from coronal plasma formed at about 1.5 MK. Repeating our combined BP analysis for images taken daily (at 00:00 UT), we can compile surveys of BP density at all heliographic longitudes and latitudes. Figure 2 shows a single-day AIA/EUVI longitude-latitude BP distribution from 22 January 2012 (Fig. 2a), together with a BP density distribution accumulated over a 28-day period on a 2°×2° longitude-latitude grid (Fig. 2b) centred on the same date. Figure 2c and d shows the pole-on projections of panel B of a 1°×1° longitude-latitude BP density distribution for the southern

and northern hemispheres, respectively. Supplementary Movies 1–4 illustrate the progression of these figure panels over the timeframe studied. Supplementary Fig. 1 shows the evolution of the BP density distribution at a heliospheric longitude of +72° and demonstrates that the BP density clusters associated with active regions are recurrent in time at the same longitude, or are persistent features for a lengthy period of time — behaviour that is repeated at all heliographic longitudes as seen in Supplementary Movie 5.

A standard diagnostic in terrestrial meteorology lies in the 'Hovmöller' diagram¹², which displays atmospheric variables for all sampled longitudes at fixed latitude (see Methods section). In Fig. 3, we show two such diagrams for the AIA/EUVI BP density distribution averaged over 2° around +15° and -22° latitude, respectively. In each panel, we see the BP density clusters tilt from left to right (east to west) over their lifetime, while there are groups of clusters, or trains, that appear to drift in the opposite direction. We note that the difference between the number of clusters present in the northern and southern activity patterns is due to the 2-year phase lag in the magnetic variability of the solar hemispheres^{13,14}.

Isolating well-defined clusters of BPs and fitting ellipses to their shape, we are able to use the tilt angle of the fitted ellipses to derive average westward phase velocities of 3.25 ± 2.25 m s⁻¹ and $2.65 \pm 1.60\,\mathrm{m\,s^{-1}}$ for clusters in the northern and southern hemispheres, respectively (see Supplementary Fig. 2). We detect no significant change of the phase velocity with latitude or time for the samples studied. For reference, we show straight lines of apparent westward phase velocity 3 m s⁻¹ (red dashed lines) on the panels of the figure that are developed from Supplementary Fig. 2. These wave phase velocities are consistent with other meandering velocities recently identified in the solar interior¹⁵ and add support to the assertion that BPs trace global-scale flows and magnetism8. The presence of such features propagating in longitude is indicative of the presence of global-scale rotationally driven wave modes in the solar interior 12,16. In this case, that is a magnetized Rossby wave, as we are observing the modulation of a rotating, convecting plasma^{5,17,18}. Indeed, a theoretical relationship between the toroidal magnetic field strength at the bottom of the solar convection zone and the 3 m s⁻¹ phase velocity of the magnetized Rossby waves⁵ would yield magnetic field strengths of the order of 4kG, consistent with that measured in the strongest of sunspots¹⁹.

Further, the clusters of BPs visible in Fig. 3 appear to demonstrate group, or wave-train, behaviour. To estimate the apparent group velocity of the BP clusters, a cross-correlation technique²⁰ is used on the Hovmöller diagrams (see Methods section). In this instance (see Supplementary Fig. 3), the method yields apparent eastward group velocities of 24.4 (±15.3) m s⁻¹ and 23.8 (±20.8) m s⁻¹ for the southern and northern hemispheres, respectively. The anti-directed phase and group velocities of the drifting motions observed are another signature of Rossby-like waves^{1,21}.

Figure 4 shows the statistical properties of the BP clusters in the samples studied above (see Methods section). The figure shows that

¹High Altitude Observatory, National Center for Atmospheric Research, PO Box 3000, Boulder, Colorado 80307, USA. ²Department of Astronomy, Yale University, PO Box 208101, New Haven, Connecticut 06520, USA. ³Department of Physics, Texas Tech University, Box 41051, Lubbock, Texas 79409, USA. ⁴Department of Astronomy, University of Maryland College Park, Maryland 20742, USA. ⁴e-mail: mscott@ucar.edu

					,
				·	
N					

LETTERS NATURE ASTRONOMY

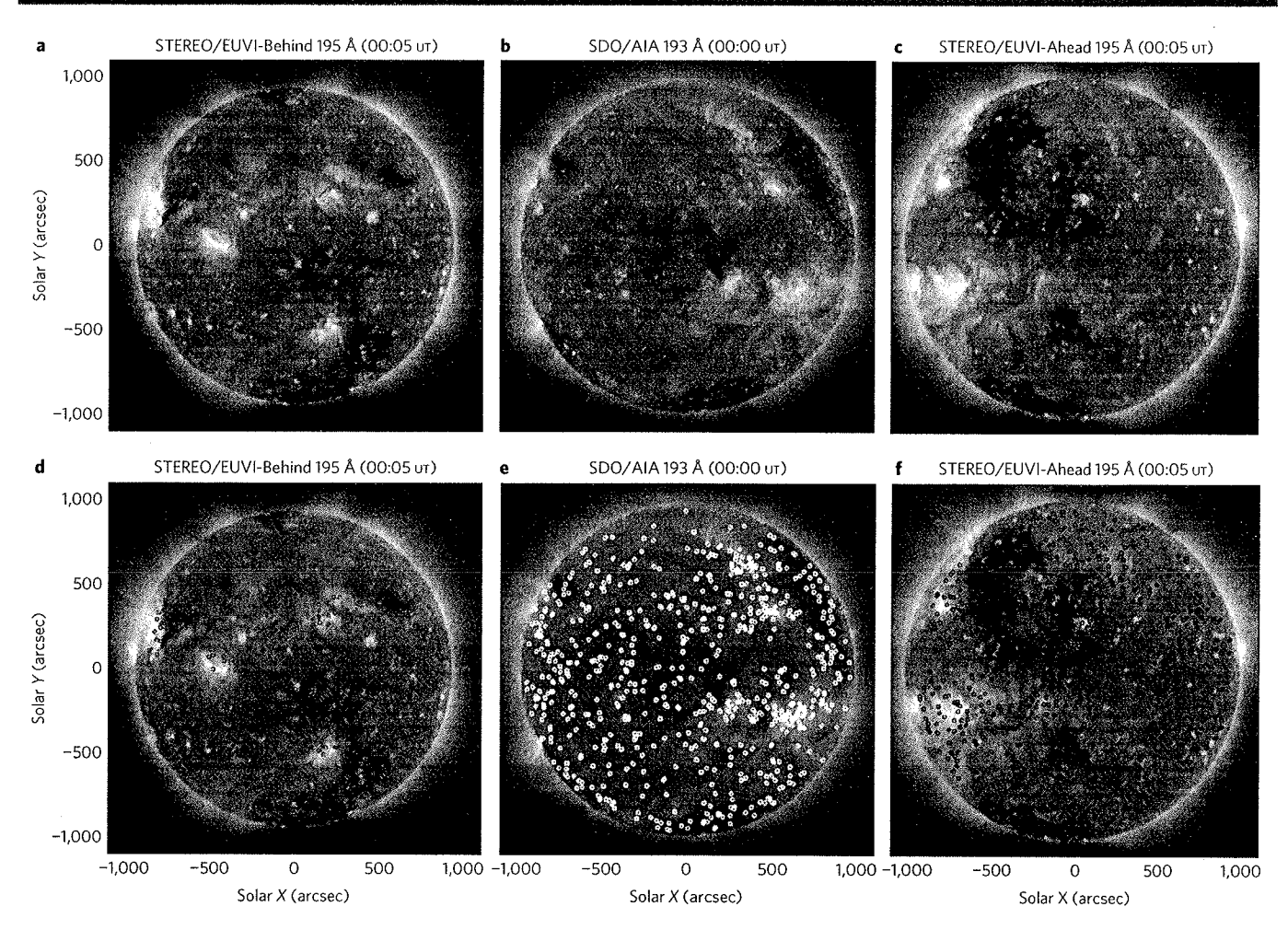


Figure 1 | Coronal BP detection at three distinct vantage points in space. BP detections by the STEREO and SDO spacecraft taken around 00:00 ut on 2 February 2011 when the entire solar corona could first be seen by all three spacecraft. The top row (**a-c**) shows coronal images from a plasma formed around 1.5 MK. The small bright concentrations seen in these images are BPs. The bottom row (**d-f**) shows the same images with respective BP detections¹⁵ shown in red (STEREO-Behind), white (SDO) and blue (STEREO-Ahead).

the well-defined BP clusters have lifetimes that appear to be integer numbers of the Sun's rotational period of 28 days, and have a mean longitudinal separation of 65° over the period of time sampled, for the latitudes shown. This whole-integer dependence of the BP cluster lifetimes when combined with the magnitude of the inferred wave phase velocity (\sim 3 m s⁻¹ westward) indicates a strong connection with seminal observational investigations of the Sun's 'torsional oscillation'^{22,23} — a long-held characteristic of the Sun's global-scale evolution and the extended solar cycle²⁴.

We have observed long-lived, slow-moving, westerly features in the combined observations of STEREO and SDO. Those wave-like patterns closely resemble the diagnostics of Rossby wave trains in the Earth's atmosphere^{12,25}. The properties determined from these combined STEREO and SDO observations would appear to intrinsically link the formation and evolution of individual solar active regions with the Rossby-like behaviour of the activity bands of the 22-year magnetic activity cycle in each solar hemisphere²⁶ and to indicate that both are driven by the rotation and the induced global circulation of our star's convective interior. Furthermore, observations of such propagating patches of strong, well-separated, recurrent magnetic activity should help to reconcile the decades of 'Rieger periodicity'27, 'active' solar longitude26,28 and 'active region nest²⁹⁻³¹ observations with their physical underpinning in the rotational forcing of the Sun's global toroidal magnetic field³² and the prevalent longitudinal wavenumbers of the underlying wave.

This finding explicitly ties the present analysis to that of previous work⁸, extending and reinforcing the spatio-temporal connection between the BP density distribution and the torsional oscillation through the magnetic bands belonging to the 22-year (extended) magnetic solar cycle. The rotational timescale dependence of BP cluster emergence and lifetimes found here also ties the present analysis to the modulation of solar activity on timescales of years and months⁶. We deduce, then, that the motions being observed are the solar analogue of a terrestrial Rossby wave — a magnetized Rossby wave — and allow us to connect the disparate timescales of solar variability.

Monitoring the wavenumber of disturbances present in the Sun's global weather patterns and understanding their magneto-hydrodynamic origins through a three-dimensional rotating stratified solar interior are critical elements to increase the predictive skill of solar activity to a level that is required to protect our technological society³³. Progress in this area requires that we adopt a continuous presence in space that provides global observations of our star, sampling all longitudes and local times, just like those that drove the advances in terrestrial meteorology in the last half of the twentieth century³⁴.

Methods

Hovmöller diagrams. The analysis presented herein relies on the extraction of information from Hovmöller diagrams¹² — a common means of plotting meteorological data to highlight the role of waves. The axes of the Hovmöller

				. *

NATURE ASTRONOMY LETTERS

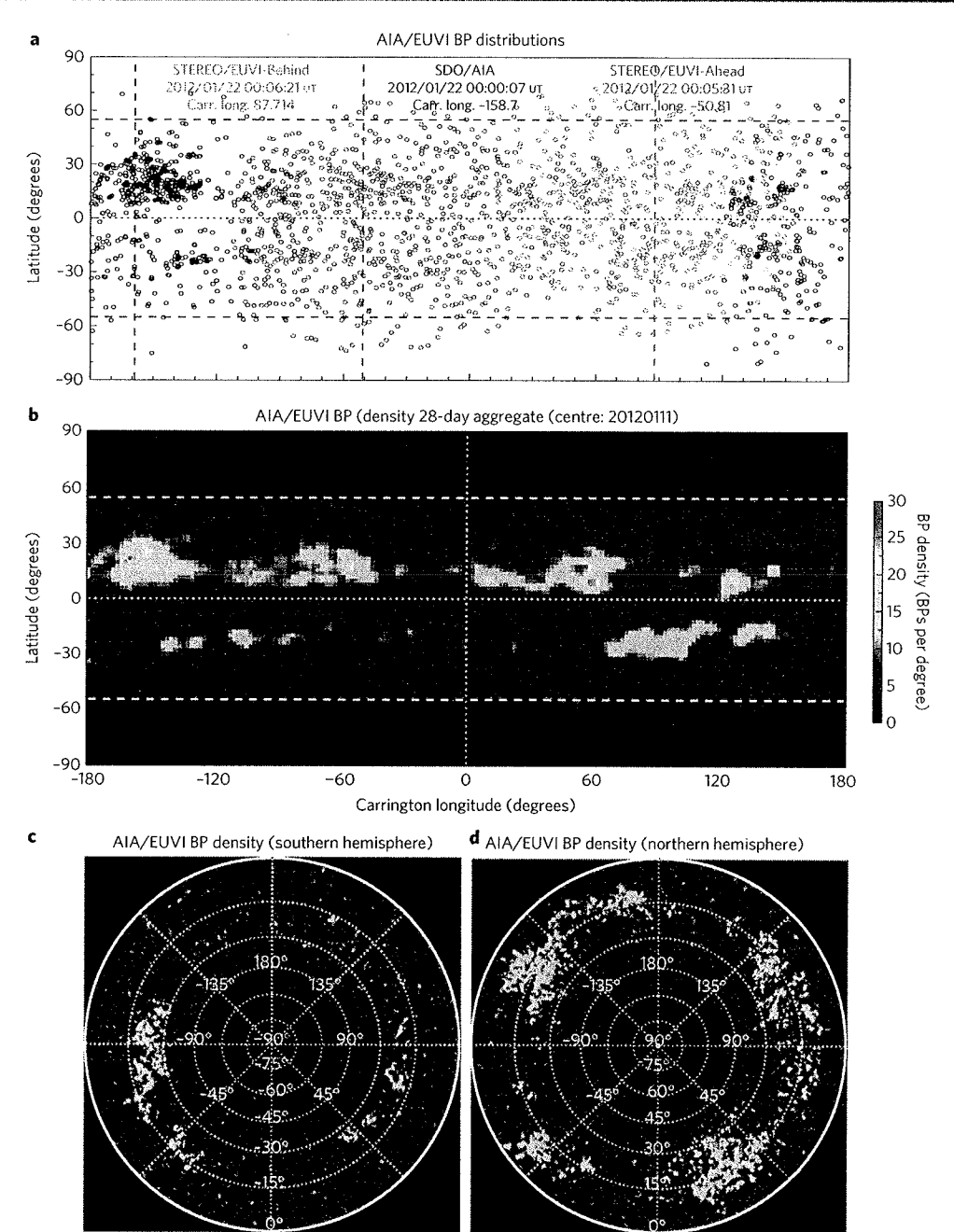


Figure 2 | Illustrating the combined coverage of BPs in the solar atmosphere from three distinct vantage points. The figure shows a longitude versus latitude snapshot of three-spacecraft BP identification and solar-rotation-averaged BP density for observations taken at 00:00 μτ on 22 January 2012.

a, BPs from SDO/AIA (black) and STEREO/EUVI (red, STEREO-Behind; blue, STEREO-Ahead). The vertical dashed lines indicate the central longitudes observed by each spacecraft. b, The comparable, 28-day averaged BP density centred on the same date (on a 2°×2° grid). c,d, The pole-on projections of the BP density (on a 1°×1° grid). Panels a and b show horizontal dashed lines at ±55° latitude and a dotted line on the equator for reference. Supplementary Movies 1-4 illustrate the temporal evolution of the panels in this figure.

diagrams presented are longitude (abscissa) and time (ordinate) for fixed latitudes. In other words, they are space–time plots that illustrate the evolution of a spherical dynamical system over a narrow range of latitudes, in which the resulting circular band of information represents the complete longitudinal evolution of the system with time. These diagrams were used to illustrate the global migration of pressure ridges and seasonal rainfall migration patterns across the world when computeraided animations of the Earth's spherical system were not possible. Slanting straight lines in a Hovmöller diagram, like any space–time plot, indicate a succession of disturbances that are propagating.

Hovmöller diagrams constructed from the combined STEREO/EUVI and SDO/AIA BP density data are shown in Fig. 3 with two dashed lines. The red dashed lines represent the apparent phase velocity of the clusters of BP density,

and the white dashed line is a representation of the group velocity of those clusters, although this dataset makes definitive determination of the latter difficult. In the following paragraphs, we will discuss the method used in the derivation of these slopes.

Wave phase velocity estimation. Estimation of the apparent phase velocity of the wave can be derived from the inclination angle of the clusters in the Hovmöller diagrams. Following the identification and isolation of distinct regions of BP density that exceed the value of 5 BP per day per degree, we numerically fit an ellipse to the enclosed cluster of points to measure their lifetime and the tilt angle subtended by the cluster to the vertical. The tilt angle provides a measure of velocity: a cluster that is parallel to the ordinate demonstrates no motion in

LETTERS NATURE ASTRONOMY

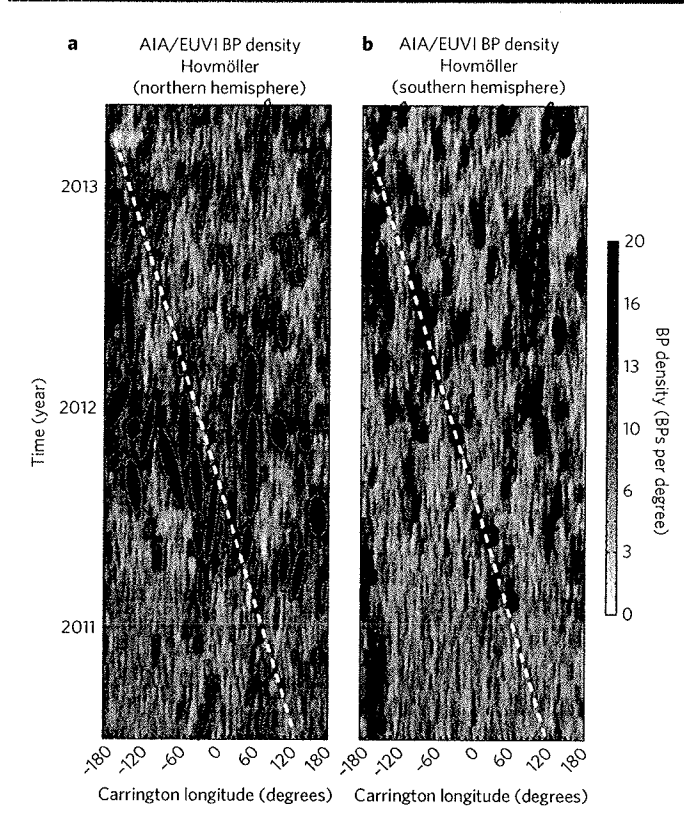
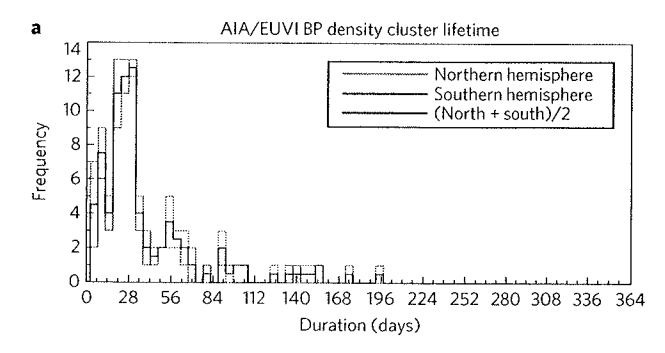


Figure 3 | Illustrating the phase and group velocities of solar Rossby waves in this sample. Hovmöller diagrams (longitude versus time at fixed latitude) are shown for the BP density distributions derived from 360° solar observations. **a**, The Hovmöller diagram for a band of latitudes 2° wide that is centred on 15° in the northern hemisphere; **b**, the corresponding Hovmöller diagram for 22° in the southern hemisphere. In both cases, we see that the clusters of enhanced BP density exhibit a westward (left-to-right) phase velocity over their lifetime, while there is an apparent eastward (right-to-left) group velocity. Analysis of the cluster shape yields a westward phase velocity of approximately 3 ms⁻¹ (red dashed reference line), whereas the analysis of their longitudinal separation yields an eastward group velocity of approximately 24 ms⁻¹ (white dashed reference line) in each hemisphere (see Methods section).

longitude, whereas a westward motion would slant from left to right and an eastward motion would slant, conversely, from right to left. In Supplementary Fig. 2, we show the fitted ellipses to the easily identified BP density clusters in the northern (red ellipses in Supplementary Fig. 2A; 95 in number) and southern solar hemispheres (red ellipses in Supplementary Fig. 2C; 67 in number) from the data presented in Fig. 3. We see that the vast majority of the clusters appear to slant left to right in both cases. To characterize the mean value of the slant of these clusters in each hemisphere, we present, in Supplementary Fig. 2B and D, histograms of the collected tilt angles (θ) converted into velocity (velocity = $\tan \theta$ = range of cluster longitude / cluster lifetime; a velocity in radians per year is easily converted into metres per second). Fitting a Gaussian function to the tilt angle distributions (thick solid line) indicates a mean velocity of 3.25 (\pm 2.25) m s⁻¹ in the northern hemisphere and 2.65 (\pm 1.6) m s⁻¹ in the southern hemisphere. These mean values are shown in the figure as thick dashed vertical lines in the corresponding panel. These slow, non-zero, motions of the BP density clusters we identify with the westward phase velocity of the waves in each hemisphere of the Sun.

There appear to be other drifting patterns in the Hovmöller diagrams, but their determination in this dataset is difficult and probably not unique. From the reference lines shown in Fig. 3, we see that the 3 m s⁻¹ (red dashed) line can allow us to associate many clusters as possibly belonging to a train; thus the disturbances could have a westward group velocity close to 3 m s⁻¹. However, there may also be eastward-travelling trains of BP density clusters (see below).

We note that it is possible to detect such small velocities in data that have a low spatial resolution, of the order of hundreds of kilometres per image pixel in all three spacecraft, because the clusters of BPs persist for so long that we are able to characterize their collective motion.



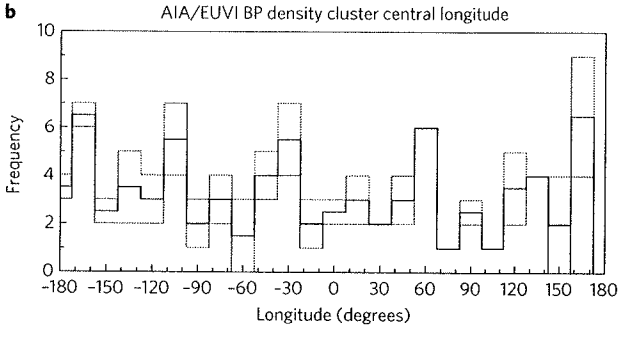


Figure 4 | Sample lifetimes and longitudinal distribution of BP clusters visible in hemispheric Hovmöller diagrams. a, Histogram of the ellipse lifetimes; **b**, central positions, for the hemispheric examples shown in Fig. 3 (see also Supplementary Fig. 1). In each case, we show the distributions for the northern hemisphere (red), southern hemisphere (blue) and their sum (black).

Cluster properties. The ellipses identified in the process above provide us with information about the lifetimes of the events that give rise to the BP clusters, presumably magnetic flux emergence from the Sun's interior, and their effect on coronal structure. In Fig. 4a, we show the histogram of cluster lifetimes, derived from the fitted ellipses. In both hemispheres, there are notable peaks at approximately 28 days and 56 days (or approximately one and two solar rotations), with the latter having about one-quarter the amplitude of the former. Similarly, we can infer (as shown in Fig. 4b) that there may be some spatial dependence in the clusters. For the sampled latitudes (and times), there appears to be a mean separation of clusters of $\sim\!65^\circ$ in each hemisphere. These values seem to indicate that the approximate wavenumber of the disturbances observed in the EUV BP density is, on average, 5. In combination, these factors will be useful in subsequent theoretical efforts to study, in more detail, the wave modes that are present.

Wave group velocity estimation. In an effort to isolate this possible eastward disturbance, we average over a slightly broader range of latitudes to build the Hovmöller diagrams shown in Supplementary Fig. 3. Here the average is over a 5° wide range of latitudes centred on 12° (northern hemisphere) and 25° (southern hemisphere) to increase signal. We then cross-correlate the time series of BP density at any reference time with that 7 days (seven time steps) later, following a prescription for identifying apparent velocities in space-time plots20. The resulting cross-correlation function has a peak at the longitude that may correspond to the staggered progression of the moving wave train. A parabolic fit to the centroid of the cross-correlation function permits an estimate of the instantaneous velocity for that time to be computed (again, velocity = longitude/time). Repeated for all time steps, we see the variation of the instantaneous velocities in Supplementary Fig. 3B and E, in which the colour-coding of the points indicates the amplitude of the fitted cross-correlation function. Supplementary Fig. 3C and F shows the histograms of the instantaneous velocities, where the cross-correlation peak is greater than 0.9. A Gaussian function is fitted to the histograms (thick red line) to reveal the mean and standard deviation of the apparent motions in the diagram for each solar hemisphere at the selected latitudes. The value of this apparent eastward-travelling motion, possibly the group velocity of the wave, is \sim 24 m s⁻¹ (24.4 ± 15.3 m s⁻¹ in the north and $23.8 \pm 20.8 \,\mathrm{m\,s^{-1}}$ in the south) and motivates the white dashed lines drawn on Fig. 3. However, we note that a dataset that could discriminate between magnetic polarities of features covering the Sun, rather than one impacting EUV brightness of the corona, could resolve this issue.

Data availability. The imaging data used in this paper are freely available from the STEREO and SDO mission archives and the Virtual Solar

NATURE ASTRONOMY LETTERS

Observatory (http://virtualsolar.org). The processed data that support the plots within this paper and other findings of this study are available from the corresponding author upon reasonable request.

Received 19 October 2016; accepted 22 February 2017; published 27 March 2017

References

- Rossby, C. G. et al. Relation between variations in the intensity of the zonal circulation of the atmosphere and the semi-permanent centers of action. J. Mar. Res. 2, 38-55 (1939).
- Lorenz, E. On the existence of extended range predictability. J. Appl. Meteorol. 12, 543–546 (1973).
- Grazzini, F. & Vitart, F. Atmospheric predictability and Rossby wave packets. Q. J. R. Meteorol. Soc. 141, 2793–2802 (2015).
- Kuhn, J. R., Armstrong, J. D., Bush, R. I. & Scherrer, P. H. Rossby waves on the Sun as revealed by solar 'hills'. *Nature* 405, 544–546 (2000).
- Zaqarashvili, T. V. et al. Long-term variation in the Sun's activity caused by magnetic Rossby waves in the tachocline. Astrophys. J. Lett. 805, 14 (2015).
- McIntosh, S. W. et al. The solar magnetic activity band interaction and instabilities that shape quasi-periodic variability. Nat. Commun. 6, 6491 (2015).
- McIntosh, S. W., Wang, X., Leamon, R. J. & Scherrer, P. H. Identifying potential markers of the Sun's giant convective scale. Astrophys. J. Lett. 784, L32 (2014).
- 8. McIntosh, S. W. et al. Deciphering solar magnetic activity. I. On the relationship between the sunspot cycle and the evolution of small magnetic features. Astrophys. J. 792, 12 (2014).
- McIntosh, S. W. & Gurman, J. B. Nine years of EUV bright points. Sol. Phys. 228, 285–299 (2005).
- Howard, R. A. et al. Sun Earth Connection Coronal and Heliospheric Investigation (SECCHI). Space Sci. Rev. 136, 67-115 (2008).
- Lemen, J. R. et al. The Atmospheric Imaging Assembly (AIA) on the Solar Dynamics Observatory (SDO). Sol. Phys. 275, 17–40 (2012).
- 12. Hovmöller, E. The trough-and-ridge diagram. Tellus 1, 62-66 (1949).
- Norton, A. A. & Gallagher, J. C. Solar-cycle characteristics examined in separate hemispheres: phase, Gnevyshev gap, and length of minimum. Sol. Phys. 261, 193–207 (2010).
- McIntosh, S. W. et al. Hemispheric asymmetries of solar photospheric magnetism: radiative, particulate, and heliospheric impacts. Astrophys. J. 765, 146 (2013).
- Hathaway, D. H., Upton, L. & Colegrove, O. Giant convection cells found on the Sun. Science 342, 1217–1219 (2013).
- Dikpati, M. & Gilman, P. A. A shallow-water theory for the Sun's active longitudes. Astrophys. J. 635, L193–L196 (2005).
- Zaqarashvili, T. V., Carbonell, M., Oliver, R. & Ballester, J. L. Magnetic Rossby waves in the solar tachocline and Rieger-type periodicities. *Astrophys. J.* 709, 749–758 (2010).
- Klimachkova, D. A. & Petrosyan, A. S. Nonlinear wave interactions in shallow water magnetohydrodynamics of astrophysical plasma. J. Exp. Theor. Phys. 122, 832–848 (2016).
- Hale, G. E. On the probable existence of a magnetic field in sun-spots. Astrophys. J. 28, 315–343 (1908).
- Tomczyk, S. & McIntosh, S. W. Time-distance seismology of the solar corona with CoMP. Astrophys. J. 697, 1384–1391 (2009).
- Dickinson, R. E. Rossby waves long period oscillations of oceans and atmospheres. Annu. Rev. Fluid. Mech. 10, 159–195 (1978).

- 22. Ulrich, R. K. Very long lived wave patterns detected in the solar surface velocity signal. *Astrophys. J.* **560**, 466–475 (2001).
- Howard, R. A. & Labonte, B. J. The Sun is observed to be a torsional oscillator with a period of 11 years. Astrophys. J. Lett. 239, 33-36 (1980).
- Wilson, P. R. *et al.* The extended solar activity cycle. *Nature* 333, 748–750 (1998).
- Glatt, I. et al. Utility of Hovmöller diagrams to diagnose Rossby wave trains. Tellus A 63, 991–1006 (2011).
- Usoskin, I. G., Berdyugina, S. V., Moss, D. & Sokoloff, D. D. Long-term persistence of solar active longitudes and its implications for the solar dynamo theory. Adv. Space Res. 40, 951–958 (2007).
- Rieger, E. et al. A 154-day periodicity in the occurrence of hard solar flares? Nature 312, 623-625 (1984).
- 28. Bumba, V. & Howard, R. A. Study of the development of active regions on the Sun. *Astrophys. J.* **141**, 1492–1501 (1965).
- Carrington, R. C. On the evidence which the observed motions of the solar spots offer for the existence of an atmosphere surrounding the Sun. Mon. Not. R. Astron. Soc. 18, 169–177 (1858).
- Castenmiller, M. J. M., Zwaan, C. & van der Zalm, E. B. J. Sunspot nests: manifestations of sequences in magnetic activity. Sol. Phys. 105, 237–255 (1986).
- Brouwer, M. P. & Zwaan, C. Sunspot nests as traced by a cluster analysis. Sol. Phys. 129, 221-246 (1990).
- Gurgenashvili, E. et al. Rieger-type periodicity during solar cycles 14–24: estimation of dynamo magnetic field strength in the solar interior. Astrophys. J. 826, 55 (2016).
- Schrijver, C. J. et al. Understanding space weather to shield society: a global road map for 2015–2025 commissioned by COSPAR and ILWS. Adv. Space Res. 55, 2745–2807 (2015).
- 34. Wexler, H. TIROS experiment results. Space Sci. Rev. 1, 7-27 (1962).

Acknowledgements

The National Center for Atmospheric Research is sponsored by the National Science Foundation and the compilation of feature databases used was supported by NASA grant NNX08AU30G. W.J.C. and M.P.M. were supported by NSF REU grant 1157020 to the University of Colorado.

Author contributions

S.W.M. contributed to data collection, data reduction, initial data analysis, manuscript writing and presentation. W.J.C. and M.P.M. contributed to data analysis and concatenation, code development and manuscript editing. R.J.L. contributed to data analysis, data interpretation and manuscript editing.

Additional information

Supplementary information is available for this paper.

Reprints and permissions information is available at www.nature.com/reprints.

Correspondence and requests for materials should be addressed to S.W.M.

How to cite this article: McIntosh, S.W., Cramer, W. J., Pichardo Marcano, M. & Leamon, R. J. The detection of Rossby-like waves on the Sun. *Nat. Astron.* **1**, 0086 (2017).

Publisher's note: Springer Nature remains neutral with regard to jurisdictional claims in published maps and institutional affiliations.

Competing interests

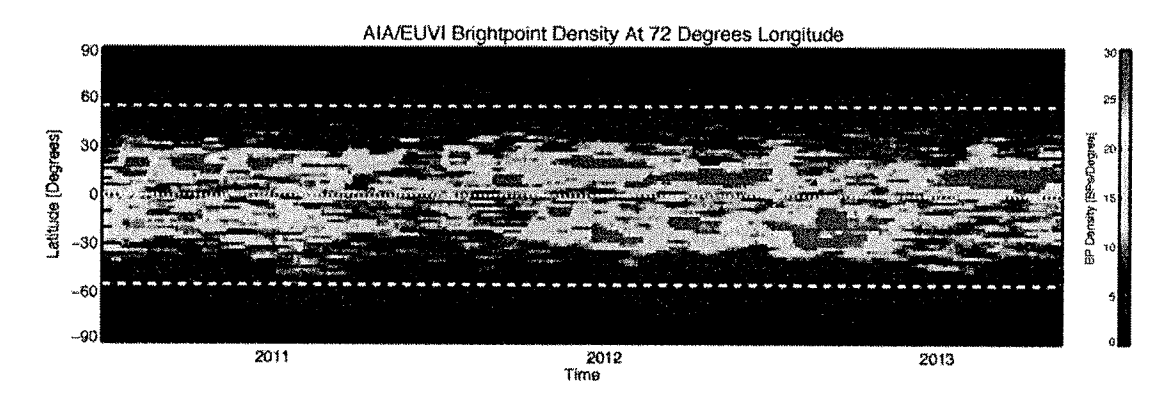
The authors declare no competing financial interests.

:			

In the format provided by the authors and unedited.

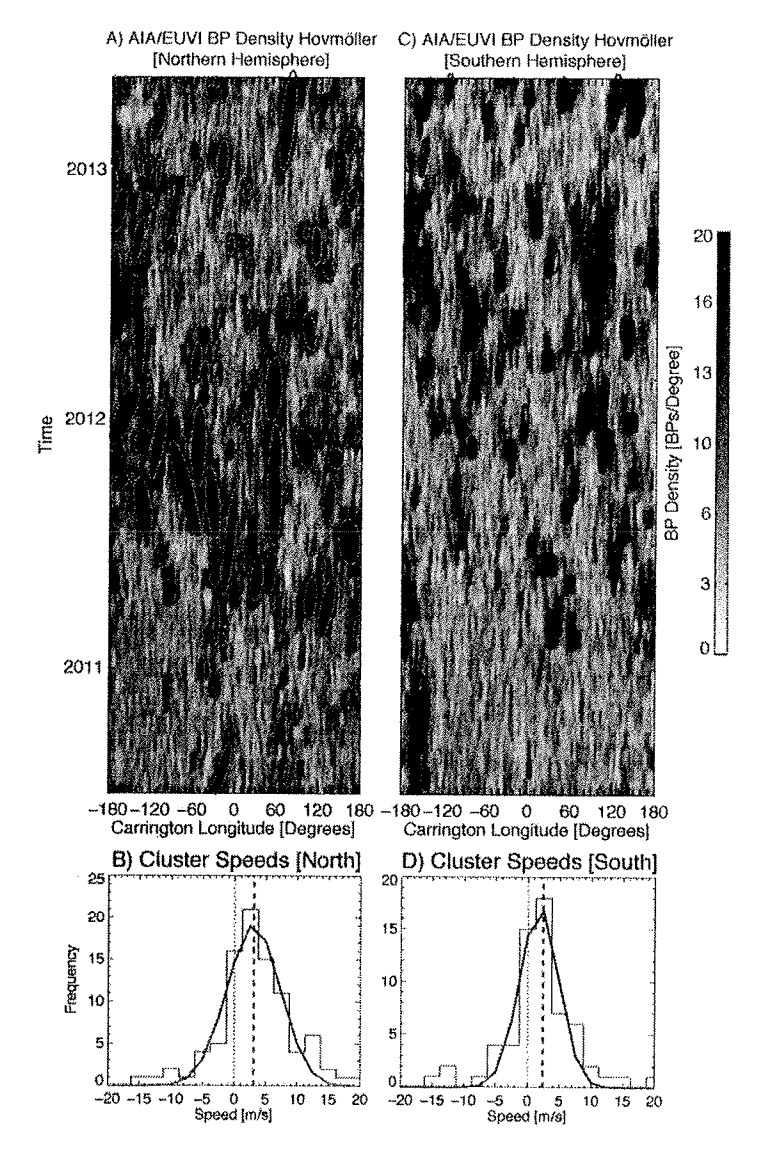
The detection of Rossby-like waves on the Sun

Scott W. McIntosh, William J. Cramer, Manuel Pichardo Marcano, Robert J. Leamon

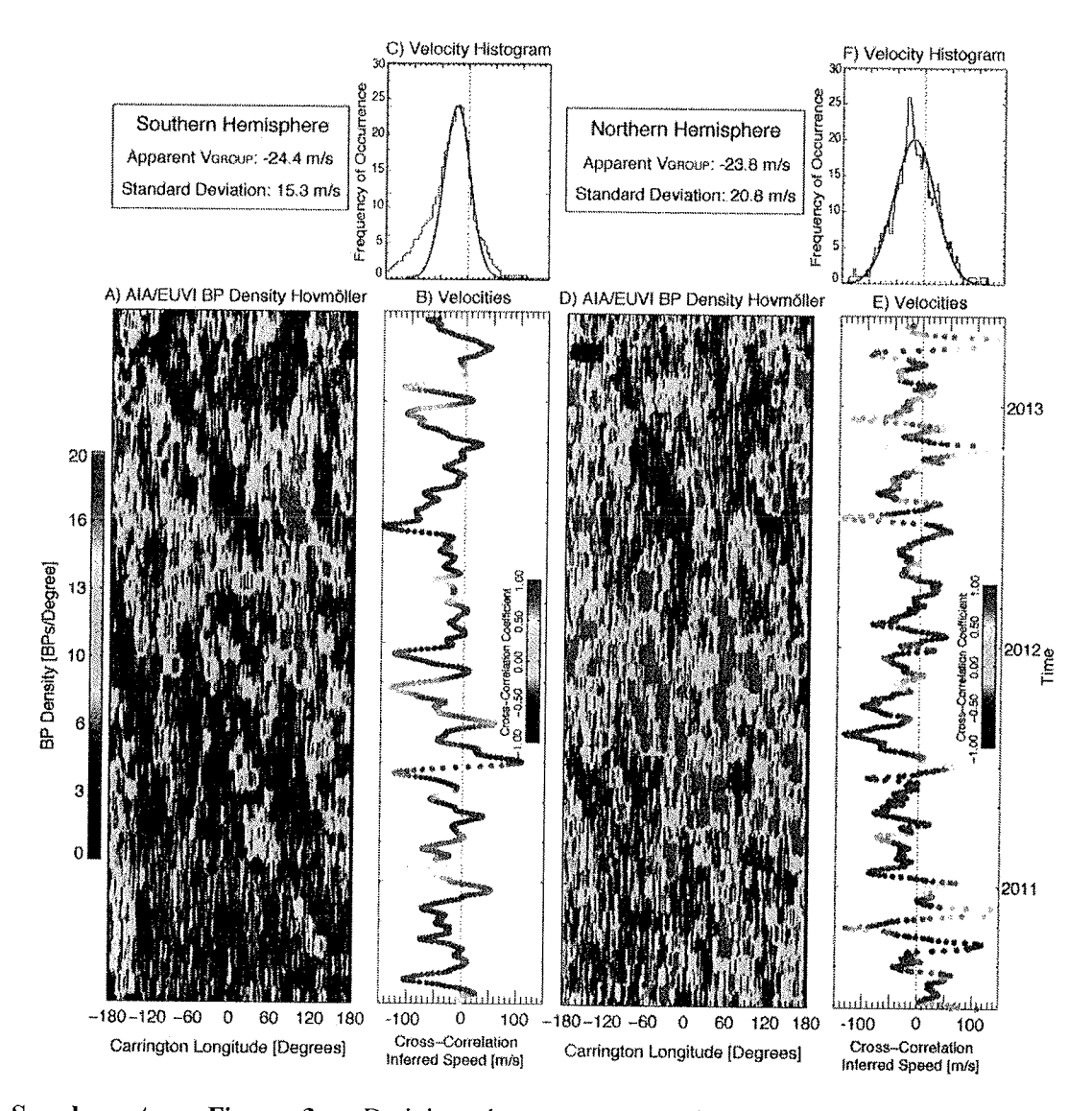


Supplementary Figure 1 - Illustrating the persistence of solar activity at given longitudes. Latitude versus time of the 28-day averaged BP density between June 1, 2010 and May 31, 2013 at a single longitude of 72°. The patches of enhanced BP density last significant periods of time. The figure shows horizontal dashed lines at $\pm 55^{\circ}$ latitude and a dotted line on the equator for reference. Supplementary Movie 5 illustrates the evolution of this plot for the range of longitudes.

		•		
,				
			. 4	

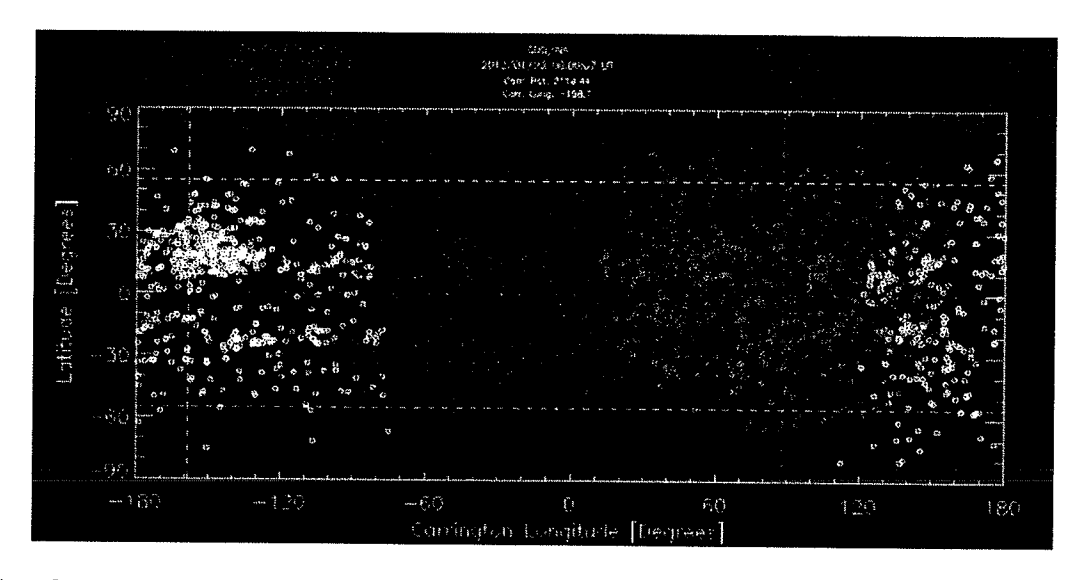


Supplementary Figure 2 - Deriving the apparent AIA/EUVI BP density cluster propagation (phase) speed for the Hovmöller diagrams of Fig. 3. In panels A and C we show the Hovmöller diagrams of Fig. 3 for the northern and southern hemispheres respectively. For each isolated cluster we represent its shape and tilt using an ellipse fitting algorithm and the resulting ellipses are shown. In panels B and D we show the corresponding histogram of ellipse tilt angles (converted to velocity - see text) as fine solid lines. The thick colored lines result from a Gaussian fit to each histogram. The vertical colored dashed line indicates the mean value of the Gaussian distribution.

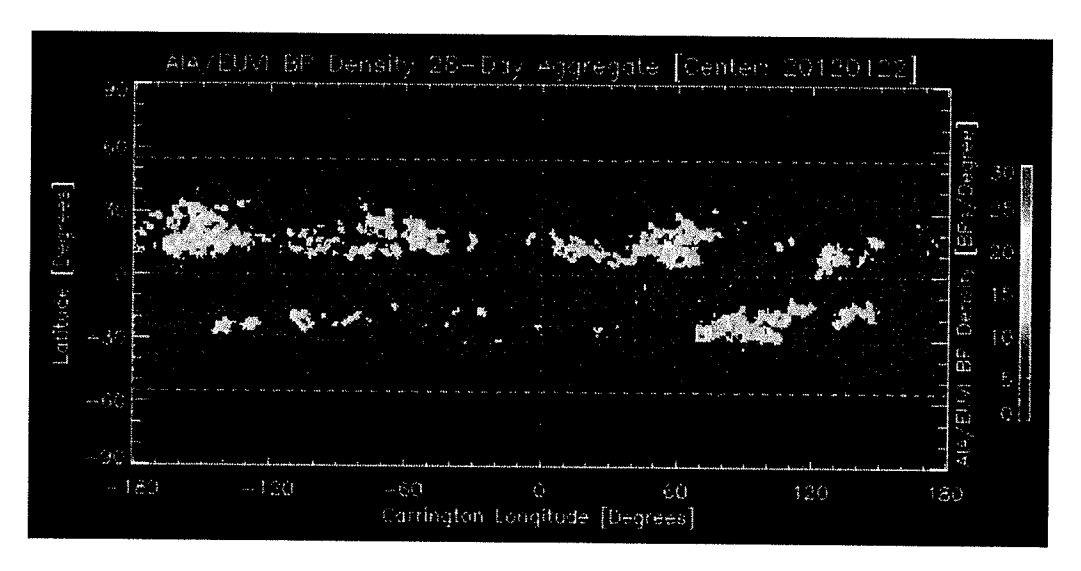


Supplementary Figure 3 - Deriving the apparent AIA/EUVI BP density cluster train propagation (group) speed from the Hovmöller diagrams of BP density of Fig. 3. In panels A and D we show Hovmöller diagrams constructed using a 5° range of latitudes centered on latitudes 12° north and 25° south respectively. Panels B and E show the corresponding cross-correlation inferred values of the velocity from the space-time diagram where the color of each datapoint represents the peak value of the cross-correlation. The histograms presented in panels C and F represent the variability of the velocities across the time period studied. A Gaussian fit to the histograms (thick red line) is made to determine the mean and standard deviation of the velocity distribution in each case.

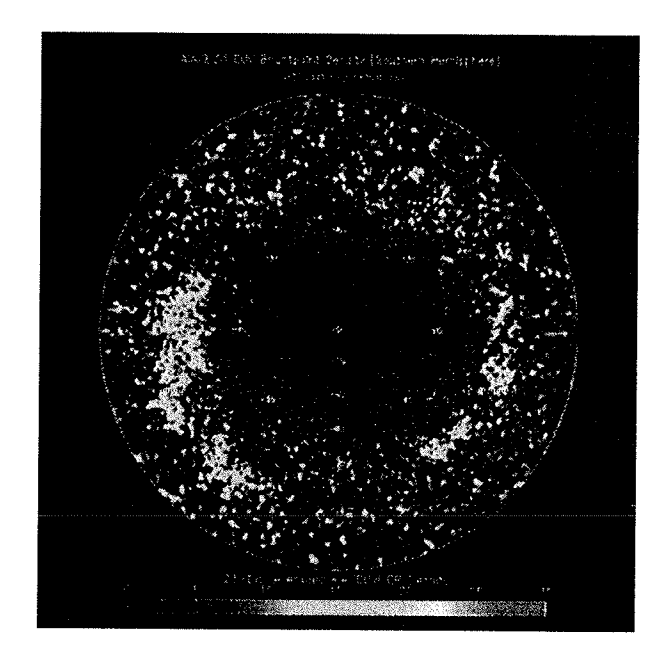
			4
	·		



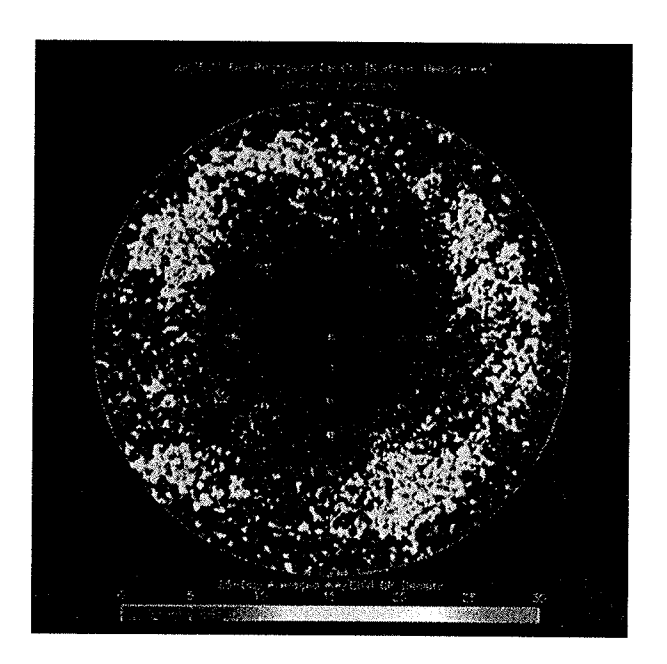
Supplementary Movie 1 - Animating the longitude versus latitude variation of the SDO/AIA and STEREO/EUVI BP identification from June 1, 2010 to May 31, 2013. We show BPs detected in SDO (white) and STEREO (red - STEREO-Behind; blue - STEREO-Ahead) observations and their evolution with time. The vertical dashed lines indicate the central longitudes observed by each spacecraft. The movie shows horizontal dashed lines at $\pm 55^{\circ}$ latitude and a dotted line on the equator for reference.



Supplementary Movie 2 - Animating the longitude versus latitude variation of the AIA/EUVI BP density distribution from June 1, 2010 to May 31, 2013. Each frame in the movie is averaged over 28-days, showing horizontal dashed lines at $\pm 55^{\circ}$ latitude and a dotted line on the equator for reference.

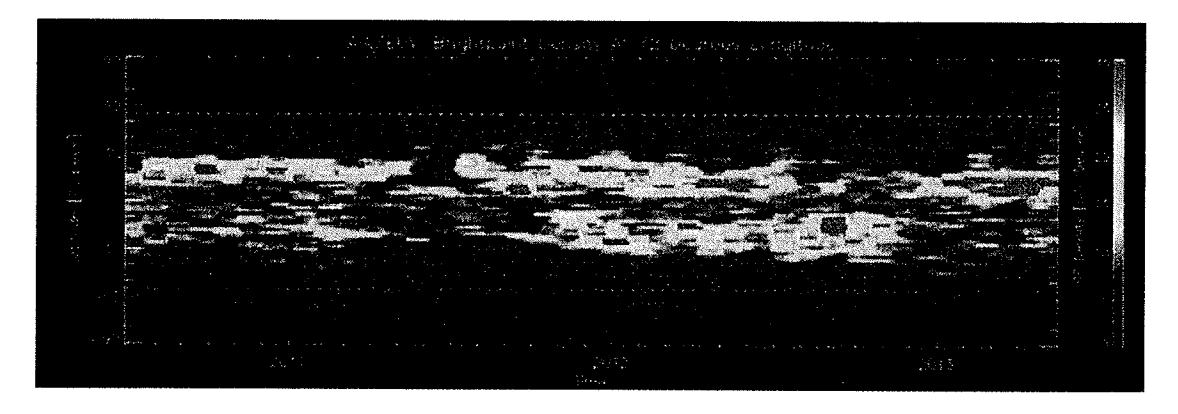


Supplementary Movie 3 - Animating the pole-on projection for the AIA/EUVI BP density distribution in the southern solar hemisphere from June 1, 2010 to May 31, 2013. Each frame in the movie is averaged over 28-days.



Supplementary Movie 4 - Animating the pole-on projection for the AIA/EUVI BP density distribution in the northern solar hemisphere from June 1, 2010 to May 31, 2013. Each frame in the movie is averaged over 28-days.

SUPPLEMENTARY INFORMATION



Supplementary Movie 5 - Animating the latitude versus time variation of the 28-day averaged AIA/EUVI BP density at different solar longitudes. The figure shows horizontal dashed lines at $\pm 55^{\circ}$ latitude and a dotted line on the equator for reference.

		,	